Cross section and heavy quark composition of $\gamma + \mu$ events produced in $p\bar{p}$ collisions

T. Affolder,[23] H. Akimoto,[45] A. Akopian,[38] M. G. Albrow,[11] P. Amaral,[8] D. Amidei,[26] K. Anikeev,[24] J. Antos,[1] G. Apollinari,[11] T. Arisawa,[45] T. Asakawa,[43] W. Ashmanskas,[8] F. Azfar,[31] P. Azzi-Bacchetta,[32] N. Bacchetta,[32] M. W. Bailey,[28] S. Bailey,[16] P. de Barbaro,[37] A. Barbaro-Galtieri,[23] V. E. Barnes,[36] B. A. Barnett,[19] S. Baroiant,[5] M. Barone,[13] G. Bauer,[24] F. Bedeschi,[34] S. Belforte,[42] W. H. Bell,[15] G. Bellettini,[34] J. Bellinger,[46] D. Benjamin,[10] J. Bensinger,[4] A. Beretvas,[11] J. P. Berge,[11] J. Berryhill,[8] B. Bevensee,[33] A. Bhatti,[38] M. Binkley,[11] D. Bisello,[32] M. Bishai,[11] R. E. Blair,[2] C. Blocker,[4] K. Bloom,[26] B. Blumenfeld,[19] S. R. Blusk,[37] A. Bocci,[38] A. Bodek,[37] W. Bokhari,[33] G. Bolla,[36] Y. Bonushkin,[6] D. Bortoletto,[36] J. Boudreau,[35] A. Brandl,[28] S. van den Brink,[19] C. Bromberg,[27] M. Brozovic,[10] N. Bruner,[28] E. Buckley-Geer,[11] J. Budagov,[9] H. S. Budd,[37] K. Burkett,[16] G. Busetto,[32] A. Byon-Wagner,[11] K. L. Byrum,[2] P. Calafiura,[23] M. Campbell,[26] W. Carithers,[23] J. Carlson,[26] D. Carlsmith,[46] W. Caskey,[5] J. Cassada,[37] A. Castro,[3] D. Cauz,[42] A. Cerri,[34] A. W. Chan,[1] P. S. Chang,[1] P. T. Chang,[1] J. Chapman,[26] C. Chen,[33] Y. C. Chen,[1] M. -T. Cheng,[1] M. Chertok,[5] G. Chiarelli,[34] I. Chirikov-Zorin,[9] G. Chlachidze,[9] F. Chlebana,[11] L. Christofek,[18] M. L. Chu,[1] Y. S. Chung,[37] C. I. Ciobanu,[29] A. G. Clark,[14] A. Connolly,[23] J. Conway,[39] M. Cordelli,[13] J. Cranshaw,[41] D. Cronin-Hennessy,[10] R. Cropp,[25] R. Culbertson,[11] D. Dagenhart,[44] S. D'Auria,[15] F. DeJongh,[11] S. Dell'Agnello,[13] M. Dell'Orso,[34] L. Demortier,[38] M. Deninno,[3] P. F. Derwent,[11] T. Devlin,[39] J. R. Dittmann,[11] A. Dominguez,[23] S. Donati,[34] J. Done,[40] M. D'Onofrio,[34] T. Dorigo,[16] N. Eddy,[18] K. Einsweiler,[23] J. E. Elias,[11] E. Engels, Jr.,[35] R. Erbacher,[11] D. Errede,[18] S. Errede,[18] Q. Fan,[37] R. G. Feild,[47] J. P. Fernandez,[11] C. Ferretti,[34] R. D. Field,[12] I. Fiori,[3] B. Flaugher,[11] G. W. Foster,[11] M. Franklin,[16] J. Freeman,[11] J. Friedman,[24] Y. Fukui,[22] I. Furic,[24] S. Galeotti,[34] A. Gallas,[16,*] M. Gallinaro,[38] T. Gao,[33] M. Garcia-Sciveres,[23] A. F. Garfinkel,[36] P. Gatti,[32] C. Gay,[47] D. W. Gerdes,[26] P. Giannetti,[34] P. Giromini,[13] V. Glagolev,[9] D. Glenzinski,[11] M. Gold,[28] J. Goldstein,[11] A. Gordon,[16] I. Gorelov,[28] A. T. Goshaw,[10] Y. Gotra,[35] K. Goulianos,[38] C. Green,[36] G. Grim,[5] P. Gris,[11] L. Groer,[39] C. Grosso-Pilcher,[8] M. Guenther,[36] G. Guillian,[26] J. Guimaraes da Costa,[16] R. M. Haas,[12] C. Haber,[23] E. Hafen,[24] S. R. Hahn,[11] C. Hall,[16] T. Handa,[17] R. Handler,[46] W. Hao,[41] F. Happacher,[13] K. Hara,[43] A. D. Hardman,[36] R. M. Harris,[11] F. Hartmann,[20] K. Hatakeyama,[38] J. Hauser,[6] J. Heinrich,[33] A. Heiss,[20] M. Herndon,[19] C. Hill,[5] K. D. Hoffman,[36] C. Holck,[33] R. Hollebeek,[33] L. Holloway,[18] R. Hughes,[29] J. Huston,[27] J. Huth,[16] H. Ikeda,[43] J. Incandela,[11] G. Introzzi,[34] J. Iwai,[45] Y. Iwata,[17] E. James,[26] M. Jones,[33] U. Joshi,[11] H. Kambara,[14] T. Kamon,[40] T. Kaneko,[43] K. Karr,[44] H. Kasha,[47] Y. Kato,[30] T. A. Keaffaber,[36] K. Kelley,[24] M. Kelly,[26] R. D. Kennedy,[11] R. Kephart,[11] D. Khazins,[10] T. Kikuchi,[43] B. Kilminster,[37] B. J. Kim,[21] D. H. Kim,[21] H. S. Kim,[18] M. J. Kim,[21] S. B. Kim,[21] S. H. Kim,[43] Y. K. Kim,[23] M. Kirby,[10] M. Kirk,[4] L. Kirsch,[4] S. Klimenko,[12] P. Koehn,[29] A. Köngeter,[20] K. Kondo,[45] J. Konigsberg,[12] K. Kordas,[25] A. Korn,[24] A. Korytov,[12] E. Kovacs,[2] J. Kroll,[33] M. Kruse,[37] S. E. Kuhlmann,[2] K. Kurino,[17] T. Kuwabara,[43] A. T. Laasanen,[36] N. Lai,[8] S. Lami,[38] S. Lammel,[11] J. I. Lamoureux,[4] J. Lancaster,[10] M. Lancaster,[23] R. Lander,[5] G. Latino,[34] T. LeCompte,[2] A. M. Lee IV,[10] K. Lee,[41] S. Leone,[34] J. D. Lewis,[11] M. Lindgren,[6] T. M. Liss,[18] J. B. Liu,[37] Y. C. Liu,[1] D. O. Litvintsev,[8] O. Lobban,[41] N. Lockyer,[33] J. Loken,[31] M. Loreti,[32] D. Lucchesi,[32] P. Lukens,[11] S. Lusin,[46] L. Lyons,[31] J. Lys,[23] R. Madrak,[16] K. Maeshima,[11] P. Maksimovic,[16] L. Malferrari,[3] M. Mangano,[34] M. Mariotti,[32] G. Martignon,[32] A. Martin,[47] J. A. J. Matthews,[28] J. Mayer,[25] P. Mazzanti,[3] K. S. McFarland,[37] P. McIntyre,[40] E. McKigney,[33] M. Menguzzato,[32] A. Menzione,[34] C. Mesropian,[38] A. Meyer,[11] T. Miao,[11] R. Miller,[27] J. S. Miller,[26] H. Minato,[43] S. Miscetti,[13] M. Mishina,[22] G. Mitselmakher,[12] N. Moggi,[3] E. Moore,[28] R. Moore,[26] Y. Morita,[22] T. Moulik,[24] M. Mulhearn,[24] A. Mukherjee,[11] T. Muller,[20] A. Munar,[34] P. Murat,[11] S. Murgia,[27] J. Nachtman,[6] V. Nagaslaev,[41] S. Nahn,[47] H. Nakada,[43] I. Nakano,[17] C. Nelson,[11] T. Nelson,[11] C. Neu,[29] D. Neuberger,[20] C. Newman-Holmes,[11] C.-Y. P. Ngan,[24] H. Niu,[4] L. Nodulman,[2] A. Nomerotski,[12] S. H. Oh,[10] Y. D. Oh,[31] T. Ohmoto,[17] T. Ohsugi,[17] R. Oishi,[43] T. Okusawa,[30] J. Olsen,[46] W. Orejudos,[23] C. Pagliarone,[34] F. Palmonari,[34] R. Paoletti,[34] V. Papadimitriou,[41] S. P. Pappas,[47] D. Partos,[4] J. Patrick,[11] G. Pauletta,[42] M. Paulini,[23,†] C. Paus,[24] L. Pescara,[32] T. J. Phillips,[10] G. Piacentino,[34] K. T. Pitts,[18] A. Pompos,[36] L. Pondrom,[46] G. Pope,[35] M. Popovic,[25] F. Prokoshin,[9] J. Proudfoot,[2] F. Ptohos,[13] O. Pukhov,[9] G. Punzi,[34] K. Ragan,[25] A. Rakitine,[24] D. Reher,[23] A. Reichold,[31] A. Ribon,[32] W. Riegler,[16] F. Rimondi,[3] L. Ristori,[34] M. Riveline,[25] W. J. Robertson,[10] A. Robinson,[25] T. Rodrigo,[7] S. Rolli,[44] L. Rosenson,[24] R. Roser,[11] R. Rossin,[32] A. Roy,[24] A. Safonov,[38] R. St. Denis,[15] W. K. Sakumoto,[37] D. Saltzberg,[6] C. Sanchez,[29] A. Sansoni,[13] L. Santi,[42] H. Sato,[43] P. Savard,[25] P. Schlabach,[11] E. E. Schmidt,[11] M. P. Schmidt,[47] M. Schmitt,[16,*] L. Scodellaro,[32] A. Scott,[6] A. Scribano,[34] S. Segler,[11] S. Seidel,[28] Y. Seiya,[43] A. Semenov,[9] F. Semeria,[3] T. Shah,[24] M. D. Shapiro,[23] P. F. Shepard,[35] T. Shibayama,[43] M. Shimojima,[43] M. Shochet,[8] J. Siegrist,[23] A. Sill,[41] P. Sinervo,[25] P. Singh,[18] A. J. Slaughter,[47] K. Sliwa,[44] C. Smith,[19] F. D. Snider,[11] A. Solodsky,[38] J. Spalding,[11] T. Speer,[14] P. Sphicas,[24] F. Spinella,[34] M. Spiropulu,[16] L. Spiegel,[11] J. Steele,[46] A. Stefanini,[34] J. Strologas,[18] F. Strumia,[14] D. Stuart,[11] K. Sumorok,[24] T. Suzuki,[43] T. Takano,[30] R. Takashima,[17] K. Takikawa,[43] P. Tamburello,[10] M. Tanaka,[43] B. Tannenbaum,[6] W. Taylor,[25] M. Tecchio,[26] R. Tesarek,[11] P. K. Teng,[1] K. Terashi,[38] S. Tether,[24] A. S. Thompson,[15] R. Thurman-Keup,[2] P. Tipton,[37] S. Tkaczyk,[11] D. Toback,[40] K. Tollefson,[37] A. Tollestrup,[11] D. Tonelli,[34] H. Toyoda,[30] W. Trischuk,[25] J. F. de Troconiz,[16] J. Tseng,[24] N. Turini,[34] F. Ukegawa,[43] T. Vaiciulis,[37] J. Valls,[39] S. Vejcik III,[11] G. Velev,[11] R. Vidal,[11] R. Vilar,[7] I. Volobouev,[23] D. Vucinic,[24] R. G. Wagner,[2] R. L. Wagner,[11] N. B. Wallace,[39] A. M. Walsh,[39] C. Wang,[10] M. J. Wang,[1] T. Watanabe,[43] D. Waters,[31] T. Watts,[39] R. Webb,[40] H. Wenzel,[20] W. C. Wester III,[11] A. B. Wicklund,[2] E. Wicklund,[11] T. Wilkes,[5] H. H. Williams,[33] P. Wilson,[11] B. L. Winer,[29]

D. Winn,[26] S. Wolbers,[11] D. Wolinski,[26] J. Wolinski,[27] S. Wolinski,[26] S. Worm,[28] X. Wu,[14] J. Wyss,[34] A. Yagil,[11] W. Yao,[23] G. P. Yeh,[11] P. Yeh,[1] J. Yoh,[11] C. Yosef,[27] T. Yoshida,[30] I. Yu,[21] S. Yu,[33] Z. Yu,[47] A. Zanetti,[42] F. Zetti,[23] and S. Zucchelli[3]

(CDF Collaboration)

[1]*Institute of Physics, Academia Sinica, Taipei, Taiwan 11529, Republic of China*
[2]*Argonne National Laboratory, Argonne, Illinois 60439*
[3]*Istituto Nazionale di Fisica Nucleare, University of Bologna, I-40127 Bologna, Italy*
[4]*Brandeis University, Waltham, Massachusetts 02254*
[5]*University of California at Davis, Davis, California 95616*
[6]*University of California at Los Angeles, Los Angeles, California 90024*
[7]*Instituto de Fisica de Cantabria, CSIC-University of Cantabria, 39005 Santander, Spain*
[8]*Enrico Fermi Institute, University of Chicago, Chicago, Illinois 60637*
[9]*Joint Institute for Nuclear Research, RU-141980 Dubna, Russia*
[10]*Duke University, Durham, North Carolina 27708*
[11]*Fermi National Accelerator Laboratory, Batavia, Illinois 60510*
[12]*University of Florida, Gainesville, Florida 32611*
[13]*Laboratori Nazionali di Frascati, Istituto Nazionale di Fisica Nucleare, I-00044 Frascati, Italy*
[14]*University of Geneva, CH-1211 Geneva 4, Switzerland*
[15]*Glasgow University, Glasgow G12 8QQ, United Kingdom*
[16]*Harvard University, Cambridge, Massachusetts 02138*
[17]*Hiroshima University, Higashi-Hiroshima 724, Japan*
[18]*University of Illinois, Urbana, Illinois 61801*
[19]*The Johns Hopkins University, Baltimore, Maryland 21218*
[20]*Institut für Experimentelle Kernphysik, Universität Karlsruhe, 76128 Karlsruhe, Germany*
[21]*Center for High Energy Physics, Kyungpook National University, Taegu, Korea 702-701,*
Seoul National University, Seoul, Korea 151-742,
and SungKyunKwan University, Suwon 440-746, Korea
[22]*High Energy Accelerator Research Organization (KEK), Tsukuba, Ibaraki 305, Japan*
[23]*Ernest Orlando Lawrence Berkeley National Laboratory, Berkeley, California 94720*
[24]*Massachusetts Institute of Technology, Cambridge, Massachusetts 02139*
[25]*Institute of Particle Physics, McGill University, Montreal, Canada H3A 2T8*
and University of Toronto, Toronto, Canada M5S 1A7
[26]*University of Michigan, Ann Arbor, Michigan 48109*
[27]*Michigan State University, East Lansing, Michigan 48824*
[28]*University of New Mexico, Albuquerque, New Mexico 87131*
[29]*The Ohio State University, Columbus, Ohio 43210*
[30]*Osaka City University, Osaka 588, Japan*
[31]*University of Oxford, Oxford OX1 3RH, United Kingdom*
[32]*Universita di Padova, Istituto Nazionale di Fisica Nucleare, Sezione di Padova, I-35131 Padova, Italy*
[33]*University of Pennsylvania, Philadelphia, Pennsylvania 19104*
[34]*Istituto Nazionale di Fisica Nucleare, University and Scuola Normale Superiore of Pisa, I-56100 Pisa, Italy*
[35]*University of Pittsburgh, Pittsburgh, Pennsylvania 15260*
[36]*Purdue University, West Lafayette, Indiana 47907*
[37]*University of Rochester, Rochester, New York 14627*
[38]*Rockefeller University, New York, New York 10021*
[39]*Rutgers University, Piscataway, New Jersey 08855*
[40]*Texas A&M University, College Station, Texas 77843*
[41]*Texas Tech University, Lubbock, Texas 79409*
[42]*Istituto Nazionale di Fisica Nucleare, University of Trieste/ Udine, Trieste, Italy*
[43]*University of Tsukuba, Tsukuba, Ibaraki 305, Japan*
[44]*Tufts University, Medford, Massachusetts 02155*
[45]*Waseda University, Tokyo 169, Japan*
[46]*University of Wisconsin, Madison, Wisconsin 53706*
[47]*Yale University, New Haven, Connecticut 06520*

We present a measurement of the cross section and the first measurement of the heavy flavor content of associated direct photon + muon events produced in hadronic collisions. These measurements come from a sample of 1.8 TeV $p\bar{p}$ collisions recorded with the Collider Detector at Fermilab. Quantum chromodynamics (QCD) predicts that these events are primarily due to the Compton scattering process $cg \rightarrow c\gamma$, with the final-state charm quark producing a muon. The cross section for events with a photon transverse momentum between 12 and 40 GeV/c is measured to be $46.8 \pm 6.3 \pm 7.5$ pb, which is two standard deviations below the most recent theoretical calculation. A significant fraction of the events in the sample contain a final-state bottom quark. The ratio of charm to bottom production is measured to be 2.4 ± 1.2, in good agreement with QCD models.

Measurements of the inclusive spectrum of direct photons in hadron-hadron collisions have provided important tests of quantum chromodynamics (QCD). Similar tests have been made with inclusive measurements of heavy flavor production (b and c quarks). The data and current perturbative QCD models do not agree well for both inclusive processes, giving insights into the possible limitations of such models [1,2]. Two previous measurements of the *associated* production of direct photons and charm quarks have provided checks of the charm quark content of the proton [3,4] through the Compton scattering process $cg \rightarrow c\gamma$. We present here an analysis with an order-of-magnitude more events, collected by the Collider Detector at Fermilab (CDF), that provides a quantitative test of perturbative QCD. In addition, this new measurement is sensitive to the production of bottom quarks in association with the photon.

The associated production of direct photons and heavy quarks in hadron collisions is expected to be a unique system for the study of the charm quark, with a 9:1 ratio of charm to bottom quarks in parton level QCD calculations [5,6]. Typically in hadron collisions, heavy quarks are produced in the gluon-gluon initiated processes $gg \rightarrow Q\bar{Q}$ and $gg \rightarrow gg \rightarrow gQ\bar{Q}$, where one of the final-state gluons splits into the heavy-quark pair. In either case if the gluon energy is sufficiently larger than the bottom quark mass, the production of bottom pairs is approximately equal to that of charm pairs. In semileptonic decays of heavy quarks, the harder fragmentation function of the bottom quark leads to its dominance in these samples (for example, a 1:4 ratio of charm to bottom in Ref. [7]). The direct-photon Compton process, however, is proportional to the quark electric charge squared, which increases the ratio of charm to bottom by a factor of 4. In addition, the intrinsic bottom quark content in the proton is 60% smaller than the charm quark content in our kinematic region. The combination of the quark charge coupling and the different proton content means the charm quark is expected to play the larger role in direct-photon events. In this paper we present the first measurement of the charm and bottom composition of direct-photon events in hadronic interactions.

The data for this analysis are from an integrated luminosity of 86 pb^{-1} of $p\bar{p}$ collisions collected with the CDF in the 1994–1995 Tevatron collider run (run 1b). The CDF detector and its coordinate system have been described in detail elsewhere [8,9]. The events in the photon data sample discussed in this paper triggered the experiment by satisfying the requirement of a photon and a muon candidate at the hardware trigger level, whereas in the previous measurements only the photon candidate was required by the trigger. This allowed a lower transverse momentum $P_T[=P\sin(\theta)]$ threshold, in this case 10 GeV. A photon candidate is selected by requiring a cluster of energy in the central electromagnetic calorimeter $|\eta_\gamma|<0.9$, with no charged tracks pointing to the cluster. The clusters are required to have a photon P_T between 12 and 40 GeV and to be isolated, with less than 1 GeV of additional transverse energy in a cone of $\Delta R = \sqrt{\Delta\phi^2 + \Delta\eta^2} = 0.4$ around the cluster. Additional photon cuts were used which were identical to those used in the run 1a CDF inclusive photon analysis [10]. Muon candidates were selected by requiring a match between a charged track with $P_T>4$ GeV/c in the central tracking chamber and a track in the appropriate muon system. For $|\eta_\mu|<0.6$, muon candidates are required to be identified in both the central muon upgrade and in the central muon upgrade system, which is behind an additional 1-m thickness of steel. For $0.6<|\eta_\mu|<1.0$ the muon candidate track was required to be reconstructed in the central muon extension system. All three muon systems are discussed in detail in Ref. [4,11]. After the track matching requirement there are 3850 events with a direct-photon candidate and a muon candidate.

Photon backgrounds from π^0 and η meson decays remain in the sample, labeled "fake $\gamma+\mu$ candidates" in Fig. 1. They are subtracted on a statistical basis using the photon background subtraction "profile" method described in Ref. [10]. This method uses the transverse energy profile of the electromagnetic shower as a discriminant between single direct photons and multiple-photon meson decays. The details of the subtraction technique are identical as in the previous analysis [10], but it has been checked in the current data sample with a clean sample of π^0's from reconstructed charged ρ decays [12]. This cross check agrees with expectations, and the systematic uncertainties determined in the previous analysis are used for this analysis as well. These uncertainties are discussed in a later section of this paper. After subtracting the photon backgrounds, 1707 ± 83 direct

_____

*Present address: Northwestern University, Evanston, IL 60208.

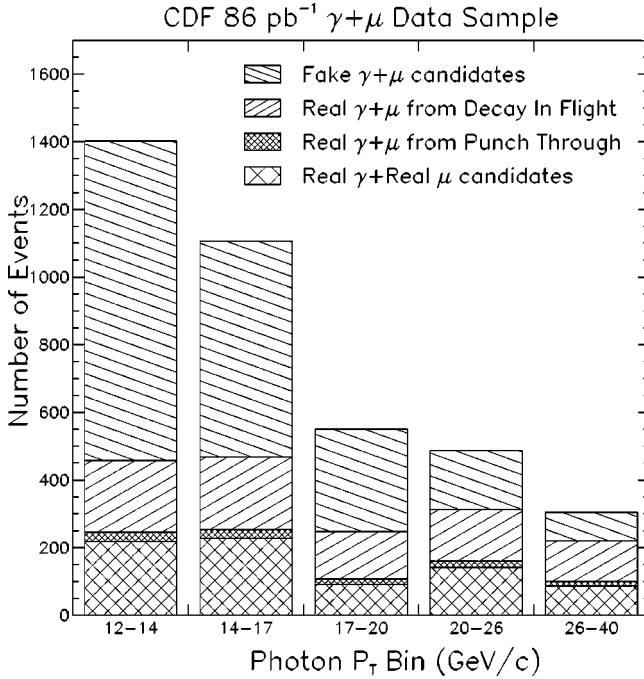†Present address: Carnegie Mellon University, Pittsburgh, PA 15213.

FIG. 1. The number of signal and background events in each bin of photon P_T are shown for the $\gamma+\mu$ sample. In addition to the signal of a real photon and a muon from a heavy-quark decay, three components of the background are shown: (1) fake photons plus real or fake muons, (2) real photons plus a muon coming from the decay of a charged pion or kaon, and (3) real photons plus a fake muon coming from the punch through of a charged pion or kaon.

FIG. 2. The probability for producing a muon with P_T >4 GeV in the semileptonic decay of a heavy quark is shown as a function of the quark P_T. These were generated using the PYTHIA Monte Carlo program to simulate the Compton $\gamma+\mu$ process. The number of muons produced in association with the photon, $N(\gamma+\mu+X)$, includes the relevant branching ratios (shown in parentheses). The quark and muon pseudorapidity are required to be within $|\eta|<1.0$. The contribution from direct and sequential decays of the bottom quark are shown, as well as the direct decay of the charm quark.

photons with a muon candidate remain. For comparison, the previous study [4] was based on 140 events.

Muon backgrounds from charged pion and kaon decays remain in this sample ("real $\gamma+\mu$ from decay in flight" in Fig. 1), as well as a smaller fraction of charged hadrons that do not interact significantly in the material in front of the muon detectors ("Real $\gamma+\mu$ from punch through" in Fig. 1). These are estimated with the same technique as in the previous analysis [4]. Starting with the parent inclusive photon + jet data sample, the four-vector of each charged particle with $P_T>0.4$ GeV/c is measured. Each track is passed into a detector simulation as a charged pion or kaon, with a π/K ratio of 60%/20% [13]. The results of the simulation are passed through the muon reconstruction; the tracks passing all cuts form the sample used for the background estimate. Backgrounds from protons that penetrate the calorimeter are negligible. After statistically subtracting the muon
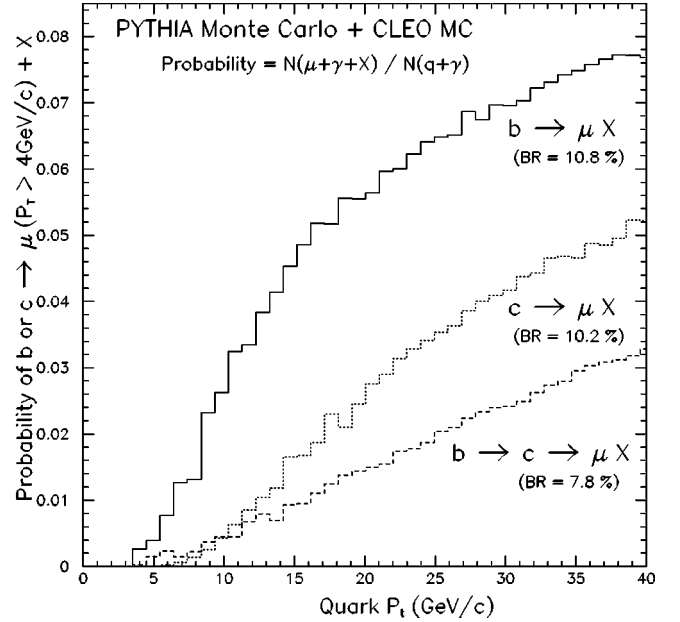
backgrounds, we expect 724 ± 89 direct-photon events with a muon that is not from charged $\pi^{\pm}$ or $K^{\pm}$ decay ("Real γ +real μ candidates" in Fig. 1). These events are assumed to come from associated direct photon + heavy-quark production with the heavy quark decaying into a muon. Figure 1 shows the number of signal and background events in five bins of photon P_T. Note that the purity of the sample improves dramatically as the photon P_T increases, which is due to the improved rejection of neutral meson backgrounds. The measured purity is consistent with that in inclusive direct-photon measurements [10].

The photon-muon cross section $d\sigma^{\gamma+\mu}/dP_T^{\gamma}$ is derived for these five bins in photon P_T by dividing by the luminosity, 86 pb^{-1}, the photon P_T bin size in GeV/c, and the efficiencies for detecting the photon within $|\eta_{\gamma}|<0.9$ and the muon within $|\eta_{\mu}|<1.0$. These efficiencies include the detector ac-

TABLE I. The measured photon-muon cross section and the predictions from PYTHIA and next-to-leading order (NLO) QCD are tabulated in five bins of photon P_T.

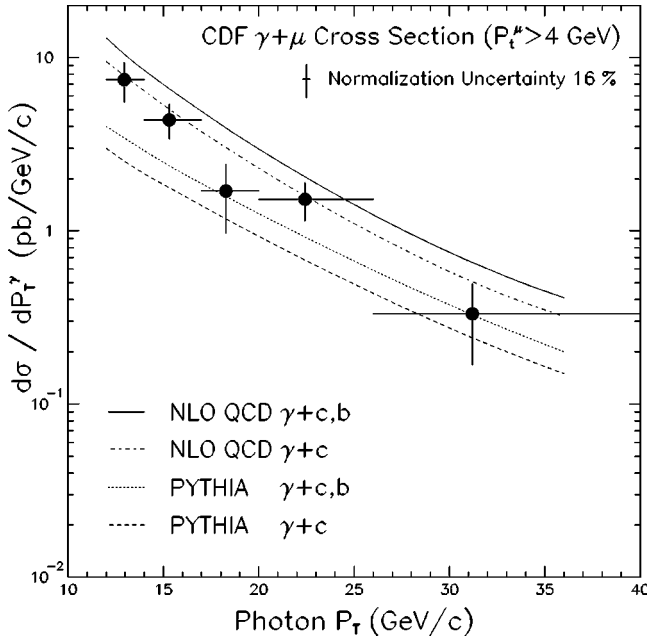| Photon P_T bin (GeV/c)	$d\sigma^{\gamma+\mu}/dP_T^{\gamma}$ (pb/GeV/c)	PYTHIA (pb/GeV/c)	NLO QCD (pb/GeV/c)
12-14	7.5 ± 1.9	3.4	10.3
14-17	4.4 ± 1.0	2.3	6.4
17-20	1.7 ± 0.7	1.5	3.8
20-26	1.5 ± 0.4	0.9	1.9
26-40	0.3 ± 0.2	0.3	0.5

FIG. 3. The measured $\gamma + \mu$ cross section is shown as a function of the photon P_T. The photon pseudorapidity is required to be within $|\eta| < 0.9$ and the muon pseudorapidity is required to be within $|\eta| < 1.0$. There is an overall 16% normalization uncertainty (not shown) on the data. The measurement is compared to QCD predictions from the PYTHIA Monte Carlo program as well as NLO QCD calculations. Both the total contribution from $\gamma + (b+c)$ and the individual $\gamma + c$ contribution are plotted.

ceptance within the relevant pseudorapidity range, but are defined after the photon or muon P_T cut. The efficiencies are measured by a combination of studies using Monte Carlo simulation and data [4,11]. The photon efficiency varies from 34% to 38% with a small photon P_T dependence, while the muon efficiency varies from 49% to 53% and depends slightly on the specific muon subsystem. The resulting photon-muon cross section is shown in Table I along with the statistical uncertainties.

There are four significant systematic uncertainties on the direct photon + muon cross section: (1) 12% from the muon background subtraction, which mostly comes from the uncertainties in the estimated pion and kaon particle fractions; (2) 7% from the photon background subtraction uncertainty, estimated in the inclusive photon measurement; (3) 7% from the uncertainty in the photon and muon cut efficiencies; and (4) 4.3% from the uncertainty in the CDF luminosity measurement, which is predominantly due to the uncertainty in the total $\bar{p}p$ cross section. These added in quadrature give an uncertainty that ranges from 16% to 20% as the photon P_T increases from 12 to 40 GeV.

The photon-muon cross section is compared to two different QCD calculations of photon-muon production. The first calculation is that in the PYTHIA [6] Monte Carlo program, which only has the leading-order (LO) contributions to the photon+heavy-quark cross section, but has the full parton shower and fragmentation effects. The CLEO heavy-quark decay tables are used [14]. The second calculation is a next-to-leading order (NLO) QCD photon+heavy flavor calcula-
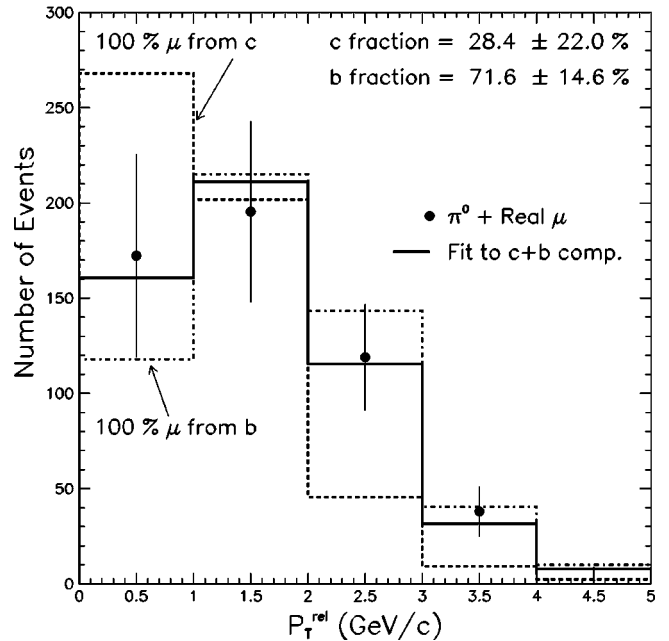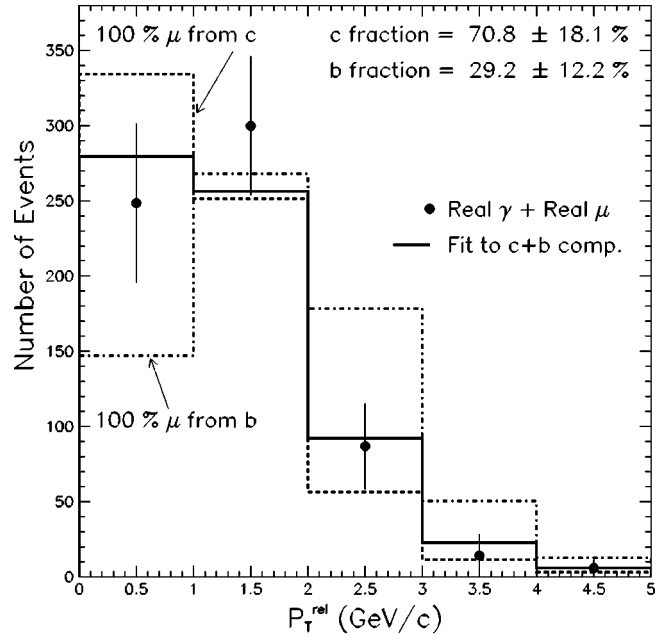

FIG. 4. The P_T^{rel} method is used to measure the sample composition of γ+heavy quark (left figure), and π^0+heavy quark (right figure). In both figures, the points are the data after subtracting the contributions from fake muons. The solid curves are the best fit to the data, the dashed curves are the expected P_T^{rel} distribution of a sample that is 100% charm, and the dotted curves are the expected P_T^{rel} distribution of a sample that is 100% bottom.

tion [5], which has additional processes not present at leading order, of which $gg \to c\bar{c} \to c\bar{c}\gamma$ is the largest contributor, but which operates only at the parton level and thus does not include heavy-quark fragmentation. For this we use the Peterson fragmentation model in PYTHIA and the CLEO decay tables. The probability of observing a 4 GeV muon from this model of the decay is shown in Fig. 2 as a function of heavy quark P_T for both direct bottom and charm decays and

for sequential decays of the bottom quark. The next-to-leading order (NLO) QCD calculation uses the massless quark approximation, which is adequate for photon+charm since the scale of the process is well above the charm mass, but cannot be applied to the photon+bottom process. The photon+bottom part of this calculation is derived from a leading-order photon+bottom calculation including mass effects, to which a multiplicative factor ("K factor," K) is then applied to account for higher-order effects. We use $K = 1.8$, which is the calculated ratio of NLO/LO in inclusive bottom production in a kinematic range that is close to that of the current measurement [15]. The uncertainties in the NLO calculation have not been thoroughly studied, but it is likely that the K factor is the largest component. If one assigns a 50% error to K, then the predicted total photon+heavy flavor NLO cross section has a 12% uncertainty. Variations of renormalization scale, parton distributions, and fragmentation functions all give variations of $\approx 5\%$.

The NLO QCD cross section, as well as the PYTHIA predictions, are compared to the data in Table I and Fig. 3. The NLO cross sections are much larger than those calculated with PYTHIA, due to the inclusion of additional processes mentioned above. The shape of the data shown in Fig. 3 matches both calculations, while the normalization is a factor 1.9 larger than the PYTHIA prediction and a factor 1.45 smaller than predicted by NLO QCD. With a data normalization uncertainty of 16% and a 12% uncertainty in the NLO QCD calculation, the data lie about two standard deviations below the NLO QCD prediction. The shape of the photon+muon cross section, however, is better described by theory than is the inclusive photon P_T spectrum. In addition, measured inclusive heavy flavor cross sections have typically been a factor of 2 larger than NLO QCD predictions [2]; we do not observe this in photon+heavy flavor production.

The current data sample is large enough to study the ratio of charm quark to bottom quark production in association with the photon. A "jet" of charged particles is measured by using the muon candidate as a seed, and then clustering charged tracks in a cone of radius 0.7 in $\eta - \phi$ space around the muon. We use the transverse momentum of the muon with respect to the jet axis, P_T^{rel}, as the variable to separate the charm and bottom fractions of the sample. The larger bottom quark mass leads to an enhanced P_T^{rel}. A maximum likelihood fit is performed to the distribution of P_T^{rel} from the photon + muon candidate sample to four template spectra: (1) photon+charm, (2) photon+bottom, (3) photon+fake muon, and (4) $\pi^0 + X$ where X is a muon candidate from any source (charm, bottom, or fake muon). The first two templates are generated using the PYTHIA Monte Carlo program [6]. The model is checked by returning to the parent photon +jet sample and comparing the P_T^{rel} distribution of the highest P_T track in the jet to the same from PYTHIA. The modeling is quite good using default PYTHIA parameters. The third template, photon+fake muon, comes from the same data +simulation combination used to estimate the fake muons for the cross section. Its normalization in the fit is constrained with a Gaussian weight using the systematic uncer-

tainty of 12% coming from the cross section measurement. The fourth template, $\pi^0 + X$, comes directly from the data as it is the component subtracted during the direct-photon background subtraction. The systematics on the maximum likelihood fit using these four templates come from uncertainties in the shape of each template. The systematic uncertainty on the photon+charm quark and photon+bottom quark templates are estimated by varying the input PYTHIA parameters. The allowed range of the parameters was determined by comparing the P_T^{rel} distribution in the parent photon+jet data sample with PYTHIA. This leads to an uncertainty of 0.2 in the charm/bottom ratio. The systematic uncertainty on the two data-driven templates, photon+fake muon and $\pi^0 + X$, is dominated by the photon subtraction method uncertainty and is 0.15 in the charm/bottom ratio. The statistical uncertainties from the maximum likelihood fit are much larger than the systematic uncertainties, being 1.1 in the charm/bottom ratio. The result of the fit to the charm/bottom ratio of the sample is 2.4 ± 1.2 (statistics+system), to be compared with the predictions of 2.9 by PYTHIA and 3.2 by NLO QCD. There is good agreement between data and theory in this ratio. The unique nature of this charm-enriched sample is confirmed, as the measured charm/bottom ratio of 2.4 is much larger than the value of 0.2 in the inclusive heavy flavor samples in Ref. [7]. The photon+muon P_T^{rel} distribution after all events with either a fake photon or muon are subtracted is shown in Fig. 4(a), compared to the templates for photon+charm and photon+bottom. The templates are normalized to the data. The photon+muon data are clearly a combination of charm and bottom, with a distribution more like the softer charm distribution. For comparison the same distribution using the π^0 + muon events from the same sample is shown in Fig. 4(b). Although QCD predictions for this process do not exist, qualitatively one would expect a larger bottom content since this process would not have the matrix-element enhancement due to the square of the electric charge of the quark, as does the photon+muon "Compton" process. The data confirm this hypothesis, albeit with limited statistics.

In summary, we present a measurement of direct-photon plus associated muon production in hadronic interactions with an order-of-magnitude more events than the previous measurement. The measurement is an interesting combination of direct-photon and heavy flavor physics, each of which has had difficulties in comparisons with NLO QCD calculations. The data agree in shape with the theoretical predictions, but fall below the theory in normalization by two standard deviations. The ratio of charm/bottom in the sample has been measured for the first time, and confirms the QCD expectation that the sample is very enriched in charm quarks compared to inclusive lepton samples in hadron collisions.

[1] U. Baur *et al.*, hep-ph/0005226.

[2] S. Frixione *et al.*, Nucl. Phys. **B431**, 453 (1994).

[3] CDF Collaboration, F. Abe *et al.*, Phys. Rev. Lett. **77**, 5005 (1996).

[4] CDF Collaboration, F. Abe *et al.*, Phys. Rev. D **60**, 092003 (1999).

[5] B. Bailey, E.L. Berger, and L.E. Gordon, Phys. Rev. D **54**, 1896 (1996), and references therein.

[6] T. Sjöstrand, cern-th/6488, and references therein. We used version 5.7 of PYTHIA.

[7] CDF Collaboration, F. Abe *et al.*, Phys. Rev. Lett. **71**, 2396 (1993); **71**, 500 (1993).

[8] CDF Collaboration, F. Abe *et al.*, Nucl. Instrum. Methods Phys. Res. A **271**, 387 (1988), and references therein. The coordinate system used in the CDF is (θ, ϕ), where θ is the polar angle relative to the proton beam as measured from the event vertex, and ϕ the azimuth. The pseudorapidity is defined as $\eta = -\ln \tan(\theta/2)$.

[9] CDF Collaboration, F. Abe *et al.*, Phys. Rev. D **50**, 2966 (1994).

[10] CDF Collaboration, F. Abe *et al.*, Phys. Rev. Lett. **68**, 2734 (1992); Phys. Rev. D **48**, 2998 (1993).

[11] R. T. Hamilton, Ph.D. thesis, Harvard University, 1996.

[12] D. Partos, Ph.D. thesis, Brandeis University, 2001.

[13] E731 Collaboration, T. Alexopoulos *et al.*, Phys. Rev. Lett. **64**, 991 (1990).

[14] See "QQ-The CLEO Event Generator," http://www.lns.cornell.edu/public/CLEO/soft/QQ.

[15] E. L. Berger and L. E. Gordon (private communication).